OPEN ACCESS Freely available online

PLoS one

Expression and Function of Serotonin 2A and 2B Receptors in the Mammalian Respiratory Network

Marcus Niebert[1,2☯], Steffen Vogelgesang[1,2☯], Uwe R. Koch[1], Anna-Maria Bischoff[1], Miriam Kron[2], Nathalie Bock[3], Till Manzke[1,2*]

1 Department of Neuro- and Sensory Physiology, Georg-August-University of Göttingen, Göttingen, Germany, **2** German Research Council Research Center for Molecular Physiology of the Brain, Göttingen, Germany, **3** Department of Child and Adolescent Psychiatry, Georg-August-University of Göttingen, Göttingen, Germany

Abstract

Neurons of the respiratory network in the lower brainstem express a variety of serotonin receptors (5-HTRs) that act primarily through adenylyl cyclase. However, there is one receptor family including 5-HT_{2A}, 5-HT_{2B}, and 5-HT_{2C} receptors that are directed towards protein kinase C (PKC). In contrast to 5-HT_{2A}Rs, expression and function of 5-HT_{2B}Rs within the respiratory network are still unclear. 5-HT_{2B}R utilizes a Gq-mediated signaling cascade involving calcium and leading to activation of phospholipase C and IP3/DAG pathways. Based on previous studies, this signal pathway appears to mediate excitatory actions on respiration. In the present study, we analyzed receptor expression in pontine and medullary regions of the respiratory network both at the transcriptional and translational level using quantitative RT-PCR and self-made as well as commercially available antibodies, respectively. In addition we measured effects of selective agonists and antagonists for 5-HT_{2A}Rs and 5-HT_{2B}Rs given intra-arterially on phrenic nerve discharges in juvenile rats using the perfused brainstem preparation. The drugs caused significant changes in discharge activity. Co-administration of both agonists revealed a dominance of the 5-HT_{2B}R. Given the nature of the signaling pathways, we investigated whether intracellular calcium may explain effects observed in the respiratory network. Taken together, the results of this study suggest a significant role of both receptors in respiratory network modulation.

Citation: Niebert M, Vogelgesang S, Koch UR, Bischoff A-M, Kron M, et al. (2011) Expression and Function of Serotonin 2A and 2B Receptors in the Mammalian Respiratory Network. PLoS ONE 6(7): e21395. doi:10.1371/journal.pone.0021395

Editor: Stuart E. Dryer, University of Houston, United States of America

Received February 28, 2011; **Accepted** May 27, 2011; **Published** July 18, 2011

Funding: This work was supported by the DFG Research Center Molecular Physiology of the Brain (CMPB; FZT 103). The funders had no role in study design, data collection and analysis, decision to publish, or preparation of the manuscript.

Competing Interests: The authors have declared that no competing interests exist.

* E-mail: tmanzke@gwdg.de

☯ These authors contributed equally to this work.

Introduction

Immunohistochemical and electrophysiological studies carried out over the previous twenty years have provided considerable evidence that serotonin (5-HT) released from caudal medullary raphé nuclei modulates respiratory network discharges in bulbar and spinal regions [1–8]. Subsequent research set out to determine which subtypes of 5-HT receptors (5-HTRs) are operative as pharmacological targets for a potential therapy to treat centrally caused breathing disturbances [9–17]. Those studies revealed that 5-HT_{1A}, 5-$HT_{2A/C}$, and 5-$HT_{4(a)}$ receptors modulate respiratory network discharge properties. These receptors represent only a fraction of the 5-HTR subtypes that modulate excitability of CNS neurons through various signaling pathways.

Amongst the 5-HTR family 5-HT_2Rs include 5-HT_{2A}, 5-HT_{2B}, and 5-HT_{2C}R isoforms that couple preferentially to $G_{q/11}$-proteins. The resulting activation of phospholipase C (PLC) increases hydrolysis of inositol phosphates and elevates cytosolic Ca^{2+} [18,19]. 5-HT_2Rs are located post-synaptically [20–22], and there is evidence that they modulate neurotransmission at various central and peripheral synaptic sites [23,24].

5-HT_{2A}Rs stimulate PLC, leading to activation of protein kinase C (PKC), and increased excitability in bulbar respiratory neurons [25–27]. Earlier studies demonstrated PKC pathway-mediated modulation of the respiratory pattern [26] and excitation of respiratory neurons by activation of 5-HT_{2A}Rs [25,27]. Beside direct modulation of the respiratory motor pattern, 5-HT_{2A}Rs may have a key role in the induction of long-term facilitation of phrenic nerve activity in response to intermittent hypoxia [28–31].

5-HT_{2B}Rs have been implicated in anxiety, schizophrenia, autism, migraine, and spreading depression [32]. In addition, 5-HT_{2B}R-dependent serotonin uptake influences the plasma serotonin level [33]. 5-HT_{2B}Rs are also important regulators of embryonic development; inactivation of the 5-HT_{2B}R gene leads to partial embryonic and early neonatal death in mice [34]. In the respiratory network, it has been shown that 5-HT_{2B}Rs enhance rhythmic motor discharge activity recorded in neonatal mice *in vitro* [35].

Until now, there were no detailed descriptions published of 5-HT_{2B}R distribution in the brainstem with expression data only available for the neocortex, cerebellum, dorsal hypothalamus, and medial amygdala [36].

In the present report, we provide a detailed account of the expression and distribution of 5-HT_{2B}Rs and 5-HT_{2A}Rs in the ponto-medullary respiratory network including respiratory motor population of the cervical spinal cord and brainstem. Using a monospecific anti-5-HT_{2B}R-antibody prepared in our laboratory and a commercially available 5-HT_{2A}R antibody, we show that 5-

HT_{2B}Rs and 5-HT_{2A}Rs are expressed in neurons of the pre-Bötzinger complex (pre-BötC), an essential kernel of the respiratory network associated with the primary rhythmogenesis [37–40].

Furthermore, our study also demonstrates that both receptors affect discharge properties in the phrenic motor output.

Materials and Methods

The experimental procedures were performed in accordance with European Community and National Institutes of Health Guidelines for the Care and Use of Laboratory Animals. The Ethics Committee of the Georg-August-University, Göttingen, Germany approved the study and assigned the approval ID **T1108** to this work.

Antibody generation

The polyclonal antibodies against the rat 5-HT_{2B}R were generated by immunizing three New Zealand White rabbits (Charles River) with a 16mer peptide derived from the second intracellular loop of the rat 5-HT_{2B}R amino acid sequence (NH_2-*CAISLDRYIAIKKPIQ*-COOH; NCBI-Accession No.: NP_058946). For immunization purposes, peptides were coupled to keyhole limpet hemocyanin (KLH) according to standard protocols. The rabbits were immunized with 300 µg of KLH-coupled peptide in Hunter's adjuvant (TiterMax Gold, Sigma) five times (28-days-intervall). The resulting antiserum was affinity-purified against the immunizing peptide.

Western Blot detection of 5-HT_{2B}R protein

Brain stem tissue isolated from both male Sprague-Dawley rats and male C57BL/6J mice were resuspended in 200 µl cell lysis buffer (50 mM Tris/HCl, pH 8.0, 150 mM NaCl, 2% w/v SDS, 1% NP40, 0.5% Na-Deoxycholate) supplemented with protease inhibitor cocktail (Sigma). Protein content was determined using a Lowry assay for high SDS concentration according to manufacturer's instructions (BioRad). 40 µg of total protein of each sample were boiled in 5× Laemmli buffer (250 mM Tris/HCl, pH 6.8; 10 mM EDTA, 10% w/v SDS, 5% v/v 2-mercaptoethanol, 50% v/v glycerol, 0.5% w/v bromophenol blue) for 5 min at 95°C and then separated using a precast SDS-PAGE (Novex). Proteins were transferred to a nitrocellulose membrane. The membrane was blocked with 4% w/v BSA/TBS/0.05%Tween (pH 7.4) for 45 min at RT. 5-HT_{2B}R protein was detected with a self-made monospecific polyclonal antibody (1:1,000 dilution) after incubation for 3 hours at RT. After extensive washing, appropriate secondary horseradish peroxidase (HRP)-conjugated antibodies (Dianova, Hamburg, Germany) were used at a dilution of 1:20,000 for 2 hours at RT. The visualization of the antigen-antibody reaction was performed with enhanced chemiluminescence (ECL) kit (BioRad, Germany).

Immunohistochemistry

(a) Preparation of brain tissue. Male juvenile Sprague-Dawley rats (P25–P32) were deeply anesthetized with isoflurane (1-Chloro-2,2,2-trifluoroethyl-difluoromethylether, Abbott, Wiesbaden, Germany) until they were unresponsive to painful stimuli (pressure applied to a forepaw). A thoracotomy was performed, and animals were transcardially perfused with 50 ml of 0.9% NaCl followed by 200 ml of 4% phosphate-buffered formaldehyde (10 ml/min). The brain was removed and post-fixed for 4 hours with the same fixative at 4°C, cryoprotected in 10% sucrose for 2 hours followed by 30% sucrose in 0.1 M phosphate buffer overnight at 4°C, and then frozen at −25°C. Series of 20- and 40-µm-thick brain sections were cut from cervical spinal cord to midbrain collicular level using a freezing microtome (Frigocut, Reichert-Jung, Germany).

(b) Peroxidase anti-peroxidase (PAP) staining. The endogenous peroxidase activity of free-floating sections was blocked with methanol/30% H_2O_2 (1:100 dilution) for 45 min at room temperature (RT) in the dark. After washing, sections were permeabilized with 0.2% Triton X-100 for 30 min. Sections were transferred for 30 min into phosphate buffered saline (PBS; pH 7.4) containing 5% bovine serum albumin (BSA) at RT for blocking non-specific binding sites. Our homemade affinity-purified rabbit anti-5-HT_{2B}R antibodies or mouse anti-5-HT_{2A}R antibodies (BD Bioscience, Cat. No.: 556326, San Diego, USA) were applied at a concentration of 2–5 µg/ml in a carrier-solution of 2% BSA/PBS. Sections were incubated with horseradish peroxidase (HRP)-conjugated anti-rabbit- or anti-mouse IgG antibodies (Dianova; 1:4,000 diluted in 2% BSA/PBS) for 1 h at RT, washed, and subsequently incubated with freshly prepared diaminobenzidine (DAB) solution for 10 min at RT. Sections were mounted onto gelatine-coated microscope slides, dehydrated in increasing ethanol concentrations (2×50%, 2×80%, 2×99.9%), cleared with four changes of xylene, and finally coverslipped with DePeX (Serva, Germany).

(c) Immunofluorescence. Sections were permeabilized with 0.2% Triton X-100 for 30 min at RT and then washed two times with PBS (pH 7.4). Non-specific binding sites were blocked with PBS containing 5% BSA for 1 h at RT. Sections were incubated with primary antibodies (2–5 µg/ml) for 4 hours at RT. After washing, sections were incubated for 2 hours at RT in the dark with species-specific Cy2- or Cy5-conjugated secondary antibodies (Dianova, Germany; 2% BSA/PBS, antibody dilution 1:400). Neuronal immunofluorescence was analyzed with a confocal laser-scanning microscope Meta-LSM 510 (Zeiss, Germany) using laser lines at 488 nm (Ar/Kr laser) and at 633 nm (He/Ne laser). Confocal images were processed by using overlays of two channels with the LSM 510 software provided by Zeiss. Digital images were taken at 2,048×2,048 dpi and were imported into Adobe Photoshop CS4, were digitally adjusted if necessary for brightness and contrast and were assembled into plates. Subsequent imaging procedures (cell counting) were performed using ImageJ (http://rsb.info.nih.gov/ij/).

Molecular Biology

(a) Generation of expression constructs. Brain tissue from one male rat at P11 was explanted and used for total RNA isolation with the OLS RNA kit (OLS, Germany) according to manufacturer's instructions. The total RNA was used in one-step RT-PCR (Invitrogen) using primer pairs for the 5-HT_{2A}R gene [*Htr2a*, F (5′-atggaaattctttgtgaagac-3′)/R (5′-tcacacacagctaacctttt-c-3′)] and 5-HT_{2B}R gene [*Htr2b*, F (5′-atggcttcatcttataaaatgtc-3′)/R (5′-ctatatgtagctgacttggtcttc-3′)], respectively. The cycling program used for RT-PCR comprised of: initial reverse transcription at 55°C for 30 min followed by denaturation at 94°C for 2 min. 40 cycles of denaturation at 94°C for 15 sec, annealing at 57°C for 30 sec, and elongation at 68°C for 90 sec were concluded with a final elongation step at 68°C for 5 min. The resulting RT-PCR fragment was purified from the gel and cloned into pTarget expression vector (Promega). Sequencing validated the correct insert identity.

(b) Transfection of cell lines. Murine neuroblastoma cell line N1E-115 was obtained from ATCC and maintained at 37°C in humid atmosphere with 5% CO_2 and passaged every second day. For transfection, cells were seeded 24 hours prior to transfection at a density of 100,000 cells in 4-well-plates (Nunc) on acid-washed and poly-L-lysine coated 12 mm round glass cover

slips. Cells were transfected with 2 µg DNA and 2 µl Lipofectamine (Invitrogen) in 500 µl OptiMEM (Invitrogen) per well and kept under normal culture conditions for 20 hours, afterwards fresh OptiMEM replaced the medium.

(c) Detection of endogenous Htr2b in cell lines by RT-PCR. Total RNA from 10^7 non-transfected cells or cells transfected with 6 µg of the plasmid encoding 5-HT_{2B}R was prepared using the OLS RNA kit. One µg of total RNA each was entered in the one-step-RT-PCR reaction, and the resulting PCR fragment was analyzed on an agarose gel. While the 5′-sequence of murine and rat *Htr2b* is identical, the 3′-sequences do differ. Therefore, for RT-PCR the rat forward primer was used, while the reverse primer for mouse was 5′-ctatatgtagctgacctgctcttc-3′.

(d) RT-PCR analyses of Htr2a and Htr2b of rat brain tissue. The total RNA of the cortex, hypoglossal nucleus, and pre-BötC dissected from corresponding 300-µm-thick slice preparations was isolated using GenElute^{TM} mammalian total RNA kit (Sigma). First strand cDNA was synthesized from 1 µg total RNA using SuperScript^{TM} first-strand synthesis system with random hexamers according to manufacturer's instructions (Invitrogen). Samples without reverse transcription (w/o RT) served as negative controls for the following PCR to exclude amplification of genomic DNA. For the PCR, specific forward and reverse primers were derived from different exons of the 5-HT_{2A}R and 5-HT_{2B}R cDNA to avoid amplification of genomic DNA. The cDNA sequences were obtained from the National Center for Biotechnology Information (NCBI; http://www.ncbi.nlm.nih.gov/). Specificity of selected primers was tested by partial sequencing of the amplification products for their identification by SeqLab company (Göttingen, Germany). The following primer pairs were used for amplification:

5-HT_{2A}R [*Htr2a*, NCBI-Accession No.: NC_005114.2; F (5′-accttgtgtgtgagtgacct-3′)/R (5′-taggccaatgctggtatagt-3′)], 5-HT_{2B}R [*Htr2b*, NC_005108.2; F (5′-ctggttattctggctgtttc-3′)/R (5′-gaccacatcagcctctattc-3′)], and for β-actin [*Actb*, NC_005111.2; F (5′-gatatcgctgcgctcgtcgtc-3′)/R (5′-cctcggggcatcggaacc-3′)].

The PCR reaction mixture for one sample was composed of 1–2 µl cDNA, 1 µl forward primer, 1 µl reverse primer, 1 µl dNTPs (100 mM dNTP mix), 1 µl DMSO, 5 µl NH_4 buffer (10×), 2 µl $MgCl_2$ (50 mM solution), and 1 µl PANScript red DNA polymerase (PAN Biotech, Germany). The mixture was filled up to 50 µl with DEPC-treated water. The following program was used for the PCR reaction: *initial denaturation* at 94°C, 4 min/38×[*denaturation* 94°C, *annealing* 1 min/55°C, *extension* 1 min/72°C, 2 min]/*final elongation* 72°C, *termination* 10 min/4°C hold. *Actb* (β-Actin) was used as an internal standard for all PCR reactions.

(e) Real-time RT-PCR. The relative quantification of *Htr2a* and *Htr2b* gene expression in specific rat tissues was done by real-time RT-PCR analysis. Spinal cord, inferior olive, pre-Bötzinger complex, and parabrachial complex were dissected from corresponding 300-µm-thick cryostat sections (P32; n = 3 animals) under visual control. The total ribonucleic acid (RNA) of homogenized brain tissue was isolated using the Trizol® method according to manufacturer's instructions (GibcoBRL) and its concentration was determined using the NanoDrop ND-1000 spectrophotometer followed by its quality and integrity measurement by electrophoresis on RNA 6000 LabChip® kit (Agilent 2100 Bioanalyzer). The RNA was transcribed into the corresponding deoxyribonucleic acid (cDNA) using the iScript cDNA Synthesis Kit (BioRad). The following primer pairs were designed by using the Primer3 program (http://frodo.wi.mit.edu/primer3/):

Htr2a (NM_017254.1): F (5′-tgtcgccatccagaacccca-3′)/R (5′-gcaggcagctcccctcctta-3′); *Htr2b* (NM_017250.1): F (5′-agactgccgagaaccagggg-3′)/R (5′-gcggtggctgatttgctggt-3′); *Hprt1* (NM_012583.2): F (5′-gtcaagcagtacagccccaaaatg-3′)/R (5′-gtttgttgttggatatgcccttgac-3′).

Gel electrophoresis revealed a single polymerase chain reaction (PCR) product, and the melting curve analysis showed a single peak for all amplification products. The PCR products were sequenced and blasted to confirm the correct identity of each amplicon. Ten-fold serial dilutions generated from cDNA of each sample were used as a reference for the standard curve calculation to determine primer efficiency. Triplicates of all real-time PCR reactions were performed in a 25 µl mixture containing 1/20 volume of the sample cDNA preparation from 250 ng total RNA, 400 nM of each primers, and 1× Fast-SYBR Green Master Mix (Applied Biosystems, USA).

The PCR-reactions were performed as follows: *initial activation* at 95°C for 60 s, 42 cycles of (*denaturation* 95°C/10 s, *annealing* and *extension* 60°C/30 s), and a final gradual increase of 0.5°C in temperature from 60°C to 90°C.

All real-time quantifications were performed using the iCycler iQ system (BioRad) and were adjusted by using the method according to Pfaffl [41].

Calcium imaging of cells recombinantly expressing 5-HT_{2A}Rs or 5-HT_{2B}Rs

The perfused brainstem preparation is, due to its thickness and need for constant perfusion not suited for microscopic analysis. Therefore, we opted to do the calcium imaging in murine neuroblastoma N1E-115 cells, where endogenous expression of 5-HT_2Rs is negligible, but are known to signal via the PLC-DAG pathway [42,43]. Another advantage of transfection is the control over which receptors (5-HT_{2A}R, 5-HT_{2B}R or both) are expressed in individual cells, avoiding the need for antagonists and simplifying analysis. 12–16 hours post transfection, cells were transferred to calcium-free imaging medium (130 mM NaCl, 3.5 mM KCl, 1.25 mM NaH_2PO_4, 24 mM $NaHCO_3$, 1.2 mM $MgSO_4$, 10 mM Glucose) and incubated with Fluo-4-AM (Invitrogen) at a final concentration of 5 µM for 30 min at 37°C. The Fluo-4-AM stock solution was prepared as 2 mM using 10% pluronic acid F-127 in DMSO (Sigma) and was diluted just before use. After incubation, cells were washed with calcium-free medium and Fluo-4-AM was allowed to hydrolyze for another 30 min in the presence of probenicid to avoid leeching of fluorescent probe from the cell.

For calcium imaging, Fluo-4-AM loaded cells were transferred to a recording chamber equipped with an inverted Olympus microscope (IX71) with appropriate filters (515 nm beam splitter and a 535/50 band-pass filter) and a triggered LED light source (PreciseExcite, CoolLED) with 465 nm excitation. Images were taken for 300 µsec at 1 sec intervals. After recording baseline fluorescence, cells were stimulated with 1000 nM serotonin (Sigma) in calcium-free medium. This concentration was chosen based on a dose-response curve giving a linear response for serotonin stimulation between 500 and 1500 nM. For all experiments, a 10×, 1.0 NA objective (Olympus) was used.

To compare calcium measurements between experiments, we calculated the apparent fluorescent intensity F/F_0 by dividing the fluorescent intensity (F) at every time point by the average fluorescence recorded before stimulation (F_0). Data were statistically analyzed with Student's t-test and presented as mean ± standard deviation (s. d.).

Perfused brainstem preparation of rats

(a) Perfused brainstem preparation of rats. The experiments on the perfused brainstem preparation [44] were performed on male Sprague-Dawley rats (P25–P32, 90–150 g)

that were housed under a 12 h light/dark cycle, with food and water provided ad libitum.

Animals were deeply anesthetized with halothane until they were unresponsive to a forepaw pinch, decerebrated at the precollicular level and cerebellectomized, bisected below the diaphragm, and the skin was removed. The upper body was placed into a recording chamber and perfused retrogradely via the thoracic aorta with ACSF (containing in mM: $MgSO_4$ 1.25; KH_2PO_4 1.25; KCl 5; NaCl 125; $CaCl_2$ 2.5; $NaHCO_3$ 25; glucose 10, 1.25% Ficoll and aerated with carbogen (5% CO_2/95% O_2; pH 7.35 at 30°C). The perfusate was collected, filtered twice and re-circulated. Norcuronium-bromide (0.5 mg/200 ml) was added for muscle relaxation. The perfusion pressure was set to 45 to 55 mm Hg.

(b) Phrenic nerve signal processing. A silver wire immersed in bath solution within a capillary suction electrode picked up phrenic nerve activity representing the respiratory motor output to the diaphragm and inspiratory rib cage muscles. Phrenic nerve signals were amplified 2,000–5,000×, filtered (low-pass, 7,000 Hz cutoff frequency; high pass, 8 Hz) and integrated (time constant, 100 ms). The processed signals were digitized by a PowerLab 8/30 microprocessor and stored using LabChart 7 software (ADInstruments, Australia).

Drugs added to the perfusate for specific pharmacological manipulation of 5-HT_2Rs were purchased from Tocris Bioscience, Ellisville, USA: 5-HT_{2A}R agonist TCB-2 and 5-HT_{2A}R antagonist Altanserin hydrochloride, 5-HT_{2B}R agonist BW 723C86 and 5-HT_{2B}R antagonist LY 272015.

(c) Analysis of phrenic nerve discharge properties. Discharges of a representative one-minute duration were measured in the absence of (control) and after intra-arterial perfusion with ACSF containing a 5-HT_{2A} or 5-HT_{2B} receptor agonist or antagonist. Measurements of drug effect were made at 5-minute intervals. The peak of the integrated discharge (mV) was used as an estimator of discharge intensity and normalized to the control, which was set to 100%. Discharge frequency (bursts per minute) was calculated from the integrated signals. Values (mean ± standard error of the mean) for amplitude and frequency were calculated from consecutive discharges that occurred over one minute during control and when drug effects were maximal.

All statistical tests (paired t-test) for pharmacological experiments were performed using GraphPad Prism version 5.0d for MacOS X.

Test drugs

5-HT receptor ligands tested for effects on phrenic nerve discharge properties were purchased from Tocris Bioscience, USA: TCB-2 (5-HT_{2A}R agonist), Altanserin hydrochloride (5-HT_{2A}R antagonist), BW 723C86 (5-HT_{2B}R agonist), LY 272015 (5-HT_{2B}R antagonist).

Results

Production and characterization of monospecific anti-5-HT_{2B}R antibodies

The peptide for immunization was derived from the second intracellular loop of the rat 5-HT_{2B}R-sequence (NH_2-*CAISL-DRYIAIKKPIQ*-COOH; fig. 1Aa). The specificity of the monospecific polyclonal anti-5-HT_{2B}R antibody was tested in three different test systems: Immunoblot analysis (n = 3) of both mouse and rat brainstem lysate revealed a specific band at 48 kDa, which is in accordance with the predicted relative molecular mass of the receptor (fig. 1Ab). Murine neuroblastoma cells recombinantly expressing rat 5-HT_{2B}R (fig. 1B) were used for specificity testing of the antibody, while the neocortex and the hypoglossal nucleus (XII) was selected to test immunohistochemistry in tissue (fig. 1C) based on previous positive results reported by Duxon [36].

The control cells faintly expressed the mouse 5-HT_{2B}R that is also recognized by the antibody because of sequence homology. After transfection with the rat receptor the antibody labeling revealed a strong fluorescent signal. Also, both brain regions selected showed strong 5-HT_{2B}R reactivity (fig. 1Bc).

The anti-5-HT_{2B}R antibody immunoreactivity on cells as well as on neurons of both regions was effectively blocked after pre-incubation of the primary antibody with a 50-fold molar excess of the peptide that was used for immunization indicating specificity. As a control, RT-PCR analysis confirmed 5-HT_{2B}R-specific mRNA expression in cells within both regions (fig. 1Cc).

Expression analysis of 5-HT_{2A} and 5-HT_{2B}Rs in the respiratory network

Prior to analysis of 5-HT_{2A}R and 5-HT_{2B}R expression at the protein level, we confirmed their expression at the RNA level. For this, we dissected specific brain stem regions (fig. 2Aa) from corresponding frozen cryostat sections of juvenile rats (P30; n = 3 in which patches of both sides of each section were combined for one sample). Conventional RT-PCR analysis revealed gene expression for 5-HT_{2A} (*Htr2a*) and 5-HT_{2B}R (*Htr2b*) in the pre-BötC at the RNA level (fig. 2Ab). However, relative quantification of gene expression using real-time RT-PCR analysis revealed a 5.3-fold stronger expression of the *Htr2a* compared to the *Htr2b* gene in the spinal cord (0.0582±0.0061 vs. 0.0110±0.0036), 11.8-fold in the inferior olive (0.1875±0.0196 vs. 0.0159±0.0016), 6.8-fold in the pre-BötC (0.0617±0.0046 vs. 0.0091±0.0024), and a 4.1-fold stronger one in the parabrachial complex (0.0671±0.0162 vs. 0.0188±0.0061) (fig. 2C).

To analyze receptor expression at the protein level within the ponto-medullary respiratory network we applied our self-made monospecific polyclonal anti-5-HT_{2B}R antibody in combination with a commercially available monoclonal anti-5-HT_{2A}R antibody (BD Bioscience, San Diego, USA). Both receptor subtypes were expressed in crucial parts of the respiratory network such as the pre-BötC and the pontine Kölliker-Fuse nucleus (fig. 3, 4). A detailed analysis of the pre-BötC, the supposed kernel essential for the generation of the primary respiratory rhythm (Smith et al., 1991), showed a strong co-expression of 5-HT_{2A}R and 5-HT_{2B}R.

We analyzed a total amount of 2136 5-HT_{2A}R-immunoreactive cells (5 sections from each animal, n = 5 animals). 1345 cells (63%) of these cells also expressed the 5-HT_{2B}R indicating strong co-expression of 5-HT_{2A}R and 5-HT_{2B}R (fig. 3).

In the dorsolateral pons expression of 5-HT_{2B}R within the parabrachial complex (PB) and Kölliker-Fuse (KF) nucleus was weak, compared to the 5-HT_{2A}R (fig. 4D–F). Contrary, the 5-HT_{2A}R showed dense expression in the KF and lateral crescent nucleus of the PB (fig. 4A–C). Both nuclei are closely linked with respiratory control. In addition more modest expression was observed in the external lateral, central, and dorsal nuclei of the PB. Curiously, both 5-HT_{2A}R and 5-HT_{2B}R showed dense expression in the internal lateral nucleus (il) of the PB (fig. 4B, E), a subnucleus of the PB-complex that is still undefined in its physiological functions.

Analysis of systemic effects of 5-HT_{2A}Rs and 5-HT_{2B}Rs on respiratory activity

The effects of systemic application of specific antagonists for 5-HT_{2A}R and 5-HT_{2B}R (Altanserin hydrochloride and LY 272015, respectively) and specific agonists for 5-HT_{2A}R and 5-HT_{2B}R

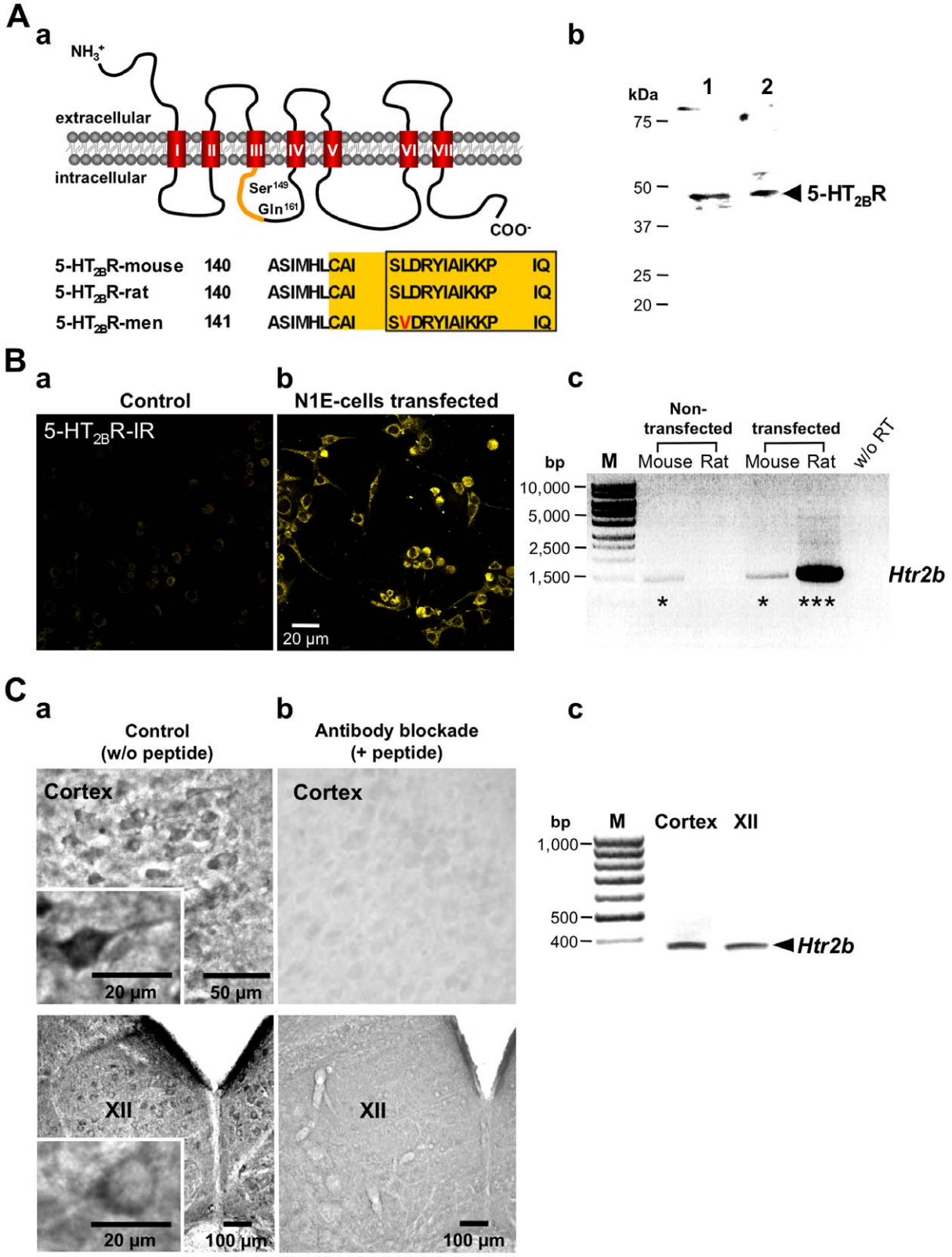

Figure 1. Verification of the anti-5-HT$_{2B}$R antibody. (**A**) (**a**) The 5-HT$_{2B}$R belongs to the family of seven-transmembrane-domain receptors that are coupled to hetero-trimeric guanine-nucleotide-binding protein q (G_q). The transmembrane-domains are indicated by red cylinders (I–VII). We produced a novel monospecific polyclonal antibody against the 5-HT$_{2B}$R by selecting a specific amino acid sequence (Cys^{146} - Gln^{161}; NH_2-*CAISLDRYIAIKKPIQ*-COOH) of the second intracellular loop of the rat 5-HT$_{2B}$R-sequence. The peptide exhibits 100% homology in mouse. Red letters indicate mismatches in the human-sequence (L→V). (**b**) Immunoblot analysis of mouse (**1**) or rat (**2**) brainstem lysate revealed a specific band at about 48 kDa that corresponds with the predicted relative molecular mass of the 5-HT$_{2B}$R. (**B**) 5-HT$_{2B}$R expression in non-transfected (**a**) and

transfected N1E-115 cells (**b**). The anti-5-HT$_{2B}$R antibody-dependent staining indicated a strong labeling of N1E-115 cells that had been transiently transfected with the rat 5-HT$_{2B}$R (**b**). Non-transfected cells expressing the mouse 5-HT$_{2B}$R showed a weak neuronal immunofluorescent signal that corresponds with a weak PCR signal (amplicon size 1114 bp) for the mouse 5-HT$_{2B}$R-mRNA (*Htr2b*) (**c**). Samples without reverse transcription (w/o RT) served as negative controls. (**C**) (**a**, **b**) Immunohistochemistry. Both pyramidal neurons of the cortex and motoneurons of the hypoglossal nucleus (XII) revealed a strong 5-HT$_{2B}$R immunoreactivity (-IR) (**a**) that was effectively blocked after pre-incubation of the antibody with a 50-fold molar excess of the peptide *CAISLDRYIAIKKPIQ* (+ peptide) that was used for immunization (**b**). Insets in (**a**) show labeled neurons at a higher magnification. Immunolabeling was performed using the PAP-method with diaminobenzidine as chromogen. (**c**) RT-PCR analysis of the rat cortex and hypoglossal nucleus. The 5-HT$_{2B}$R-specific mRNA (*Htr2b*) was detectable in neurons within both the rat cortex and the hypoglossal nucleus (XII) (amplicon size 380 bp).
doi:10.1371/journal.pone.0021395.g001

(TCB-2 and BW 723C86, respectively) on spontaneous breathing activity were investigated in male Sprague-Dawley rats using the perfused brainstem preparation [44]. We found that pharmacological manipulation of 5-HT$_2$Rs can either change the amplitude or the frequency of the phrenic nerve activity (PNA).

Application of the 5-HT$_{2A}$R-antagonist Altanserin hydrochloride (8.0 µg/ml, n = 3) [32,45] significantly reduced the amplitude from control of 100% to 52.34±4.72% ($p<0.01$), while breathing frequency increased from control of 10.25±0.63 to 14.50±3.59 bursts/min; n.s. (fig. 5A). Blockade of 5-HT$_{2B}$R with the antagonist LY 272015 (2.87 µg/ml, n = 3) [35,46] did not significantly changed both the amplitude (100% of control vs. 96.54±2.36%; n.s.) and frequency (13.50±1.32 bursts/min of control vs. 14.50±1.32 bursts/min; n.s.) (fig. 5B). Application of the 5-HT$_{2A}$R-agonist TCB-2 (0.67 ng/ml, n = 5) [47] caused an increase of the amplitude (from 100% of control to 121.3±8.99; n.s.), while respiratory frequency slightly decreased (13.67±1.45 bursts/min of control vs. 11.00±1.12 bursts/min; n.s.). Administration of the 5-HT$_{2A}$R-antagonist Altanserin caused a further decrease of frequency to 8.33±0.88; $p<0.05$; (fig. 6A). Application of the 5-HT$_{2B}$R-agonist BW 723C86 (0.67 µg/ml, n = 5) [32] only caused an increase in frequency (13.33±1.45 bursts/min of control vs. 21.00±1.73 bursts/min; $p<0.05$), while the amplitude was not affected (from 100% of control to 95.67±3.76%; n.s.). Blockade of the 5-HT$_{2B}$R using LY 272015 diminished respiratory frequency nearly to baseline level (14.00±2.08 bursts/min; $p<0.01$) (fig. 6B). Interestingly, the simultaneous application of both agonists together resulted only in an increase of frequency (from 12.33±2.03 to 17.00±2.31 bursts/min; $p<0.01$), whereas no increment of amplitude could be observed (100% of control vs. 97.33±0.67%; n.s.; fig. 6C).

Calcium imaging of cells recombinantly expressing 5-HT$_{2A}$R or 5-HT$_{2B}$R

The electrophysiological recordings showed a frequency increase controlled by 5-HT$_{2B}$Rs when both receptors were stimulated concomitantly (fig. 5C), although both 5-HT$_{2A}$R and 5-HT$_{2B}$R are coupled to the same G$_q$-mediated signaling pathway (fig. 7A).

To analyze the calcium signaling of both receptors, we expressed them recombinantly either alone or together in neuroblastoma cells. To avoid artifacts, relatively low amounts of DNA were transfected to avoid overexpression.

The recombinant approach allowed us to image single cells and correlate resulting signals to a defined complement of receptors, which would have not been possible in perfused brainstem preparations.

In neuroblastoma cells expressing 5-HT$_{2A}$Rs and 5-HT$_{2B}$Rs alone, either agonist evoked a release of cytosolic Ca^{2+} from intracellular stores (see figure 7 and table 1) with a large initial calcium spike. While the reactions of individual cells varied slightly, the mean Ca^{2+} increase of cells expressing 5-HT$_{2A}$R (peak F/F$_0$ of 2.59±0.8) was similar to those expressing 5-HT$_{2B}$R (peak

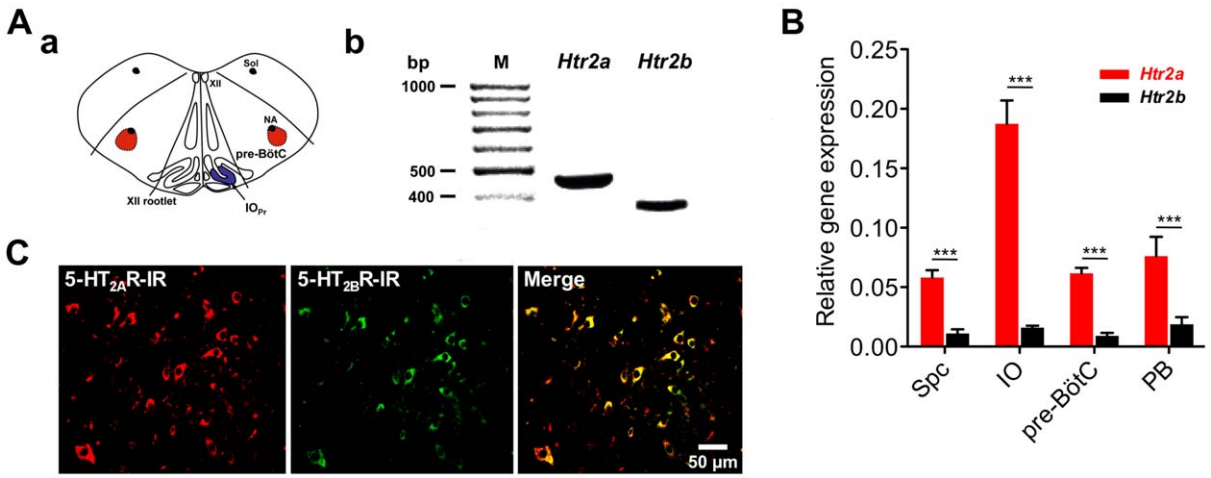

Figure 2. Quantification of expression levels and co-expression of 5-HT$_{2A}$ and 5-HT$_{2B}$Rs within the pontine respiratory network. (**A**) (**a**) shows a schematic representation of the dissected pre-BötC and its landmarks: pre-Bötzinger complex (pre-BötC), nucleus of the solitary tract (Sol), nucleus ambiguus (NA), hypoglossal nucleus (XII), principal nucleus of the inferior olive (IO$_{Pr}$). (**b**) shows the specific mRNA of both receptors detected in the pre-BötC. (**B**) Double labeling of 5-HT$_{2A}$ and 5-HT$_{2B}$Rs. 5-HT$_{2A}$ (Cy5, red) and 5-HT$_{2B}$Rs (Cy2, green) are strongly co-expressed in pre-BötC-neurons. Immunohistochemical analysis does not reveal the ratio of co-expressed proteins. Therefore, we performed quantitative real-time RT-PCR on four selected nuclei of the respiratory network (**C**). The bar diagram represents results of quantitative real-time RT-PCR analysis of 5-HT$_2$R genes (*Htr2a*, *Htr2b*) of spinal cord (Spc), inferior olive (IO), pre-Bötzinger complex (pre-BötC), and parabrachial complex (PB). At the RNA level 5-HT$_{2A}$R is significantly stronger expressed compared to *Htr2b* in all regions analyzed. Asterisks indicate significance (*** = $p<0.001$; ANOVA with Bonferroni's post hoc test).
doi:10.1371/journal.pone.0021395.g002

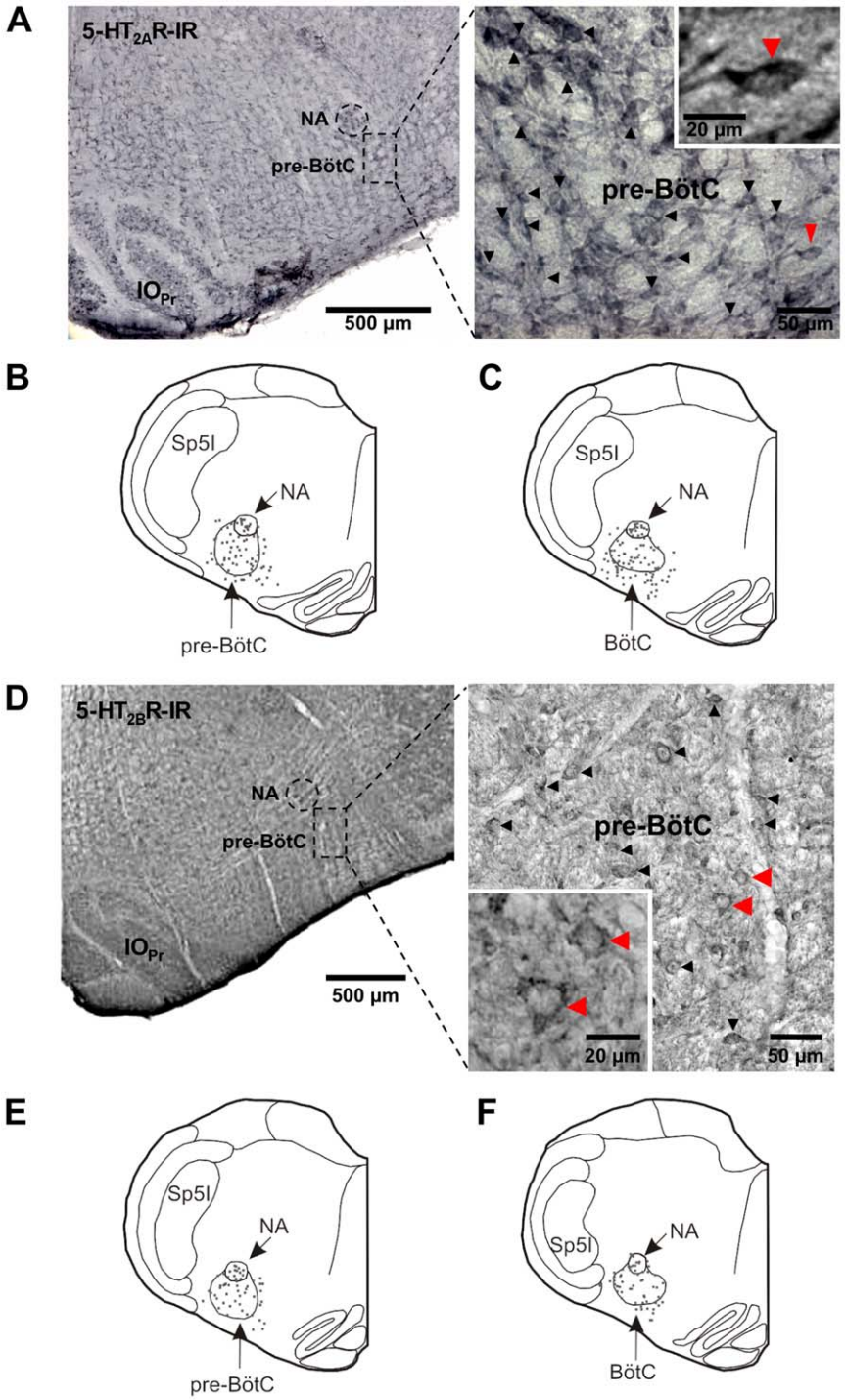

Figure 3. Expression patterns of 5-HT$_{2A}$ and 5-HT$_{2B}$Rs within the medullary respiratory network. (**A**) 5-HT$_{2A}$R expression pattern in the pre-BötC. The plots (**B**, **C**) represent 5-HT$_{2A}$R immunoreactivity within the pre-BötC (**B**) and BötC (**C**). (**D**–**F**) shows the corresponding expression pattern for the 5-HT$_{2B}$R. The insets show labeled neurons at a higher magnification. Abbreviations: Bötzinger complex (BötC), nucleus ambiguus (NA), pre-Bötzinger complex (pre-BötC), principal nucleus of the inferior olive (IO$_{Pr}$), interpolar spinal trigeminal nucleus (Sp5I).
doi:10.1371/journal.pone.0021395.g003

F/F_0 of 2.23±1.1). In contrast, the calcium increase was significantly faster for 5-HT$_{2A}$R (time to peak 30.5±9.6) than for 5-HT$_{2B}$R (time to peak 57.7±8.4). The calcium level almost returned to baseline levels within ~35 seconds exhibiting no significant differences for both receptors, with a half-peak-width of 36.7±1.7 sec for 5-HT$_{2A}$R and 34.6±3.2 for 5-HT$_{2B}$R (fig. 7B).

Co-application of 5-HT$_{2A}$R and 5-HT$_{2B}$R agonists had unexpected effects. The Ca^{2+} signal (79.44±8.9 sec) was significantly slower from onset to peak than the signals produced by either agonist alone ($p<0.001$), while the time of onset was similar to 5-HT$_{2A}$R alone. In addition, the fluorescence signal at its peak (F/F_0, 1.44±0.17) was notably smaller ($p<0.001$). While the

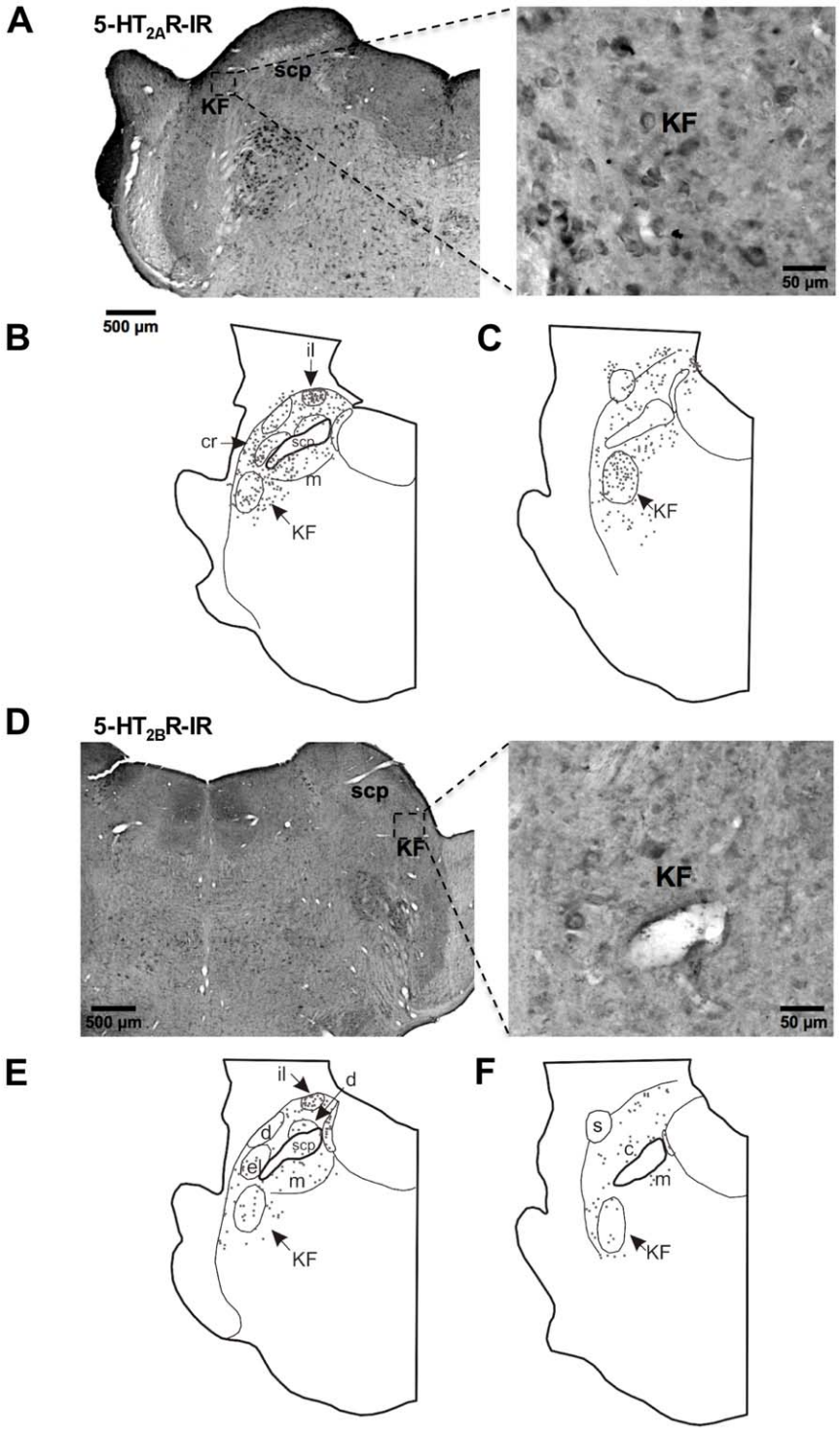

Figure 4. Expression patterns of 5-HT_{2A} and 5-HT_{2B}Rs within the pontine respiratory network. Both 5-HT_{2A} and 5-HT_{2B} receptors are abundantly expressed in neurons of the internal lateral nucleus of the parabrachial complex (**B**, **E**). Within the nucleus Kölliker-Fuse the 5-HT_{2B}R expression is weak compared to 5-HT_{2A}Rs (**A**, **D**). Abbreviations: internal lateral nucleus of the PB (il), lateral crescent nucleus of the PB (cr), nucleus Kölliker-Fuse (KF), parabrachial complex (PB), superior cerebellar peduncle (scp).
doi:10.1371/journal.pone.0021395.g004

duration of the calcium peak by co-stimulation of both receptors was nearly doubled (half-peak-width of 86.32±5.0 sec; $p<0.001$), the amount of released calcium, measured as "area under the curve", was very similar no matter if the receptors are expressed alone or together.

As our real-time PCR analysis showed that 5-HT_{2A}R and 5-HT_{2B}R are expressed in different amounts, with 5-HT_{2A}R being in 5- to 10-fold excess, we also transfected N1E cells with DNA ratios of 5-HT_{2A}R to 5-HT_{2B}R of 5:1 and 1:5, respectively. Regardless of the DNA ratios, the presence of 5-HT_{2B}R always

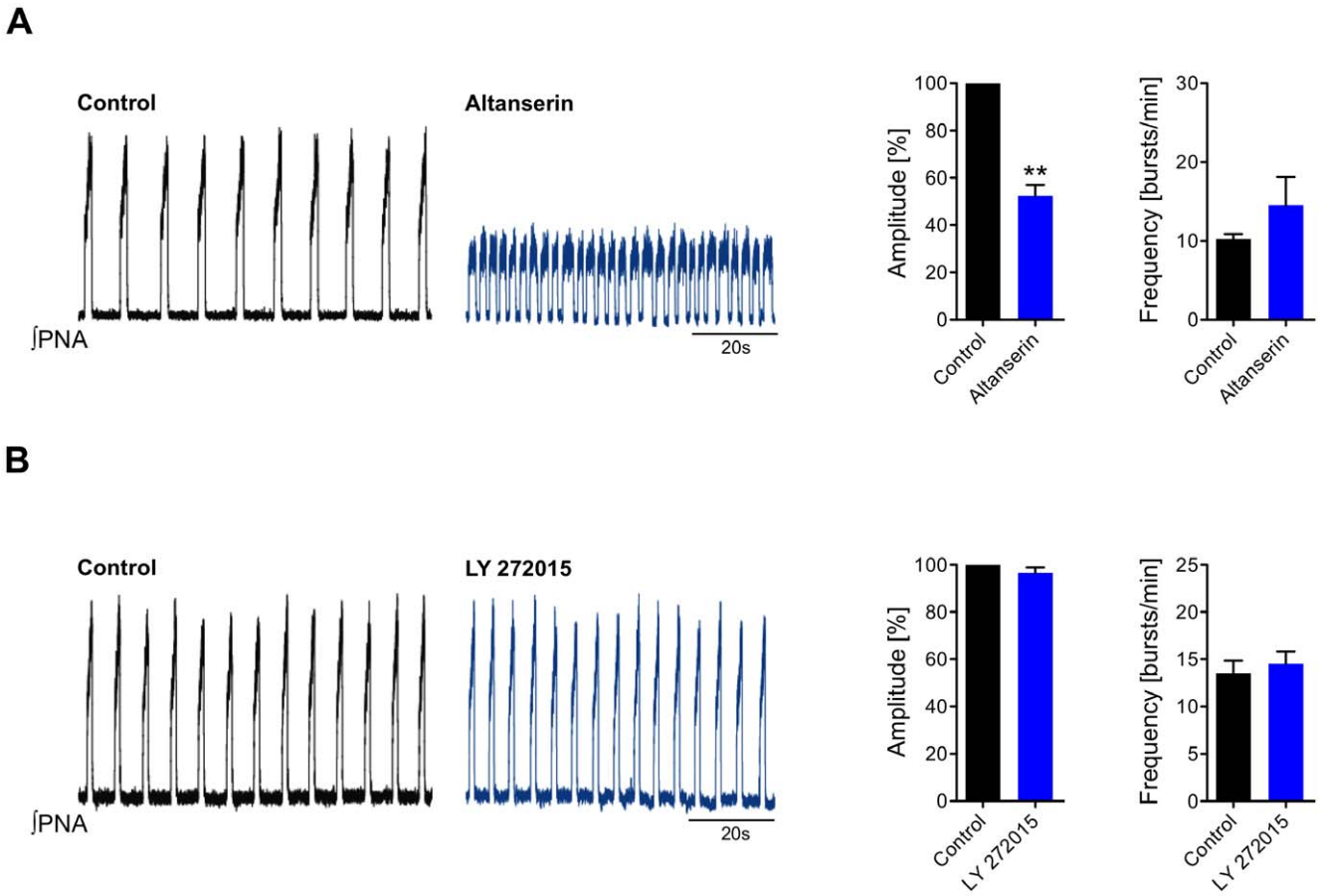

Figure 5. Respiratory network responses to systemic 5-HT$_{2A}$R and 5-HT$_{2B}$R antagonist applications of in situ rats. Shown are representative traces of integrated phrenic nerve activity (∫PNA) of 2 different experimental conditions. Black traces represent the ∫PNA under control conditions and blue traces indicate application of antagonists. The bar diagrams on the right give the averages of amplitude and frequency of least 3 independent experiments of each condition. Statistical analysis (paired t-test) is denoted in the panels on the right side with asterisks indicating significance (** = $p<0.01$). (**A**, **B**) Action of 5-HT$_{2A}$R and 5-HT$_{2B}$R antagonists in the perfused brainstem preparation of rat. (**A**) Application of the specific 5-HT$_{2A}$R antagonist Altanserin (blue trace) significantly decreased phrenic nerve activity (PNA) by decreasing the amplitude. Also, a slight increase in frequency was observed. (**B**) Application of the 5-HT$_{2B}$R antagonist LY 272015 had no discernable effect on either amplitude or frequency of ∫PNA. We interpret these findings as constitutive activity of 5-HT$_{2A}$R.
doi:10.1371/journal.pone.0021395.g005

produced slow but wide calcium transients (as shown for 5-HT$_{2A}$R and 5-HT$_{2B}$R in fig. 7C).

Discussion

This study reveals the locations of 5-HT$_{2A}$R and 5-HT$_{2B}$R in regions of the ponto-medullary respiratory network, including sites where the receptors are co-expressed. We demonstrate that agonist activation of the receptors evokes dramatic changes in discharge activity recorded from the phrenic motor output, and that activation of each type of receptor has distinctive effects on phrenic nerve discharge intensity and duration. Through the use of selective receptor antagonists, we found that only the 5-HT$_{2A}$R constitutively modulates phrenic motor output. In neuroblastoma cells transfected with 5-HT$_{2A}$R and 5-HT$_{2B}$R, we discovered distinctly different calcium signal kinetics when each type of 5-HT receptor was activated. We also uncovered unexpected effects on signal amplitude and time course when 5-HT$_{2A}$R and 5-HT$_{2B}$R are coactivated.

In the paragraphs to follow, we discuss each of these aspects in turn, along with their physiological implications for respiratory motor output modulation.

Distribution of 5-HT$_{2B}$ and 5-HT$_{2A}$ receptors in regions of the ponto-medullary respiratory network

Within the medulla and pons, functionally defined respiratory regions provide input to cranial motoneurons controlling the airways, and to spinal motoneurons activating inspiratory and expiratory pump muscles. A variety of neurotransmitters and modulators involved in respiratory control have been identified in many of these respiratory related compartments (reviewed by Alheid and McCrimmon [48]). In all these regions, 5-HT$_{2A}$R and coupled protein kinase dependent signaling pathways have been identified functionally and anatomically [49]. Until now, however, the distribution of 5-HT$_{2B}$Rs had not been investigated, and nothing had been known about their functional importance to respiratory control. Our study shows that 5-HT$_{2A}$R and 5-HT$_{2B}$R are co-localized in the Kolliker-Fuse and Parabrachial regions of the Pons, and in the BötC and pre-BötC of the ventral medulla with an approximate 5-fold stronger expression of 5-HT$_{2A}$R in all regions.

Respiratory neurons in the PB and KF constitute the pontine respiratory group. A variety of respiratory neuronal types are found in this region [50,51], which receives axonal projections from the ventral respiratory column, and from the nucleus of the solitary tract (NTS). The NTS itself is a receiving station for

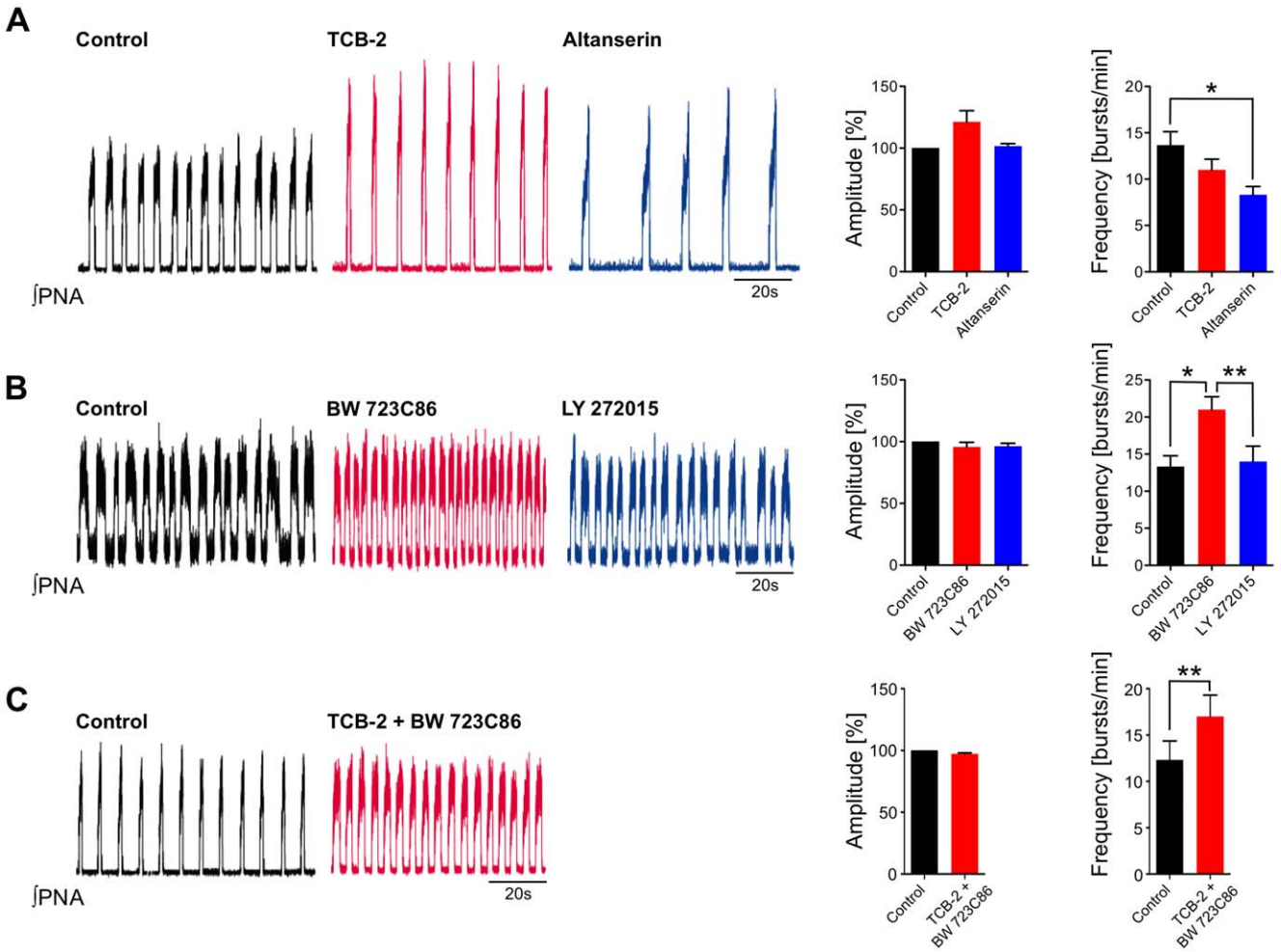

Figure 6. Respiratory network responses to systemic 5-HT$_{2A}$R and 5-HT$_{2B}$R activation. Shown are representative traces of integrated phrenic nerve activity (∫PNA) of 3 different experimental conditions. Black traces represent the ∫PNA under control conditions, while red traces indicate application of agonists and blue traces indicate application of antagonists. The bar diagrams on the right give the averages of amplitude and frequency of least 3 independent experiments of each condition. Statistical analysis (paired t-test) is denoted in the panels on the right side. (**A**–**C**) Action of 5-HT$_{2A}$R and 5-HT$_{2B}$R ligands in the perfused brainstem preparation. (**A**) Application of the specific 5-HT$_{2A}$R agonist TCB-2 (red trace) increased phrenic nerve activity (PNA) by increase of the amplitude, and subsequent application of the specific 5-HT$_{2A}$R-antagonist Altanserin (blue trace) reduced the amplitude. PNA frequency decreased below control. (**B**) Application of the 5-HT$_{2B}$R agonist BW 723C86 increased PNA frequency. After subsequent administration of the specific 5-HT$_{2B}$R-antagonist LY 272015 phrenic nerve activity returned nearly to baseline level. (**C**) Simultaneous application of the specific agonists TCB-2 and BW 723C86 only increased the frequency.
doi:10.1371/journal.pone.0021395.g006

pulmonary afferents from the lungs and upper airways. Based on 5-HT$_{2A}$R and 5-HT$_{2B}$ R co-expression patterns, our study would predict contributions by both types of receptors to respiratory modulation within the KF-PB complex, with a modulatory role played by 5-HT$_{2B}$Rs.

Based on both *in vitro* and *in vivo* [52,53] studies, the pre-BötC was identified as a medullary region essential for respiratory rhythm generation. The region may play a prominent role in inspiratory phase control, although the pre-BötC contains populations of neurons that exhibit a variety of respiratory related discharge patterns (Schwarzacher et al., 1995). Previously, 5-HT$_{1A}$, 5-HT$_{2A}$, 5-HT$_{4}$, and 5-HT$_{7}$ receptors have been identified in the pre-BötC by immuno-labeling [8,12,17]. The BötC houses a prominent population of expiratory neurons that provide widespread inhibitory projections within the ventral respiratory column (VRC), targeting both inspiratory and expiratory bulbospinal neurons as well as respiratory-related cranial motoneurons [54]. Some expiratory BötC neurons also send axon collaterals to the spinal cord, reaching at least as far as the phrenic motor nucleus [48,55]. Our present study of 5-HT$_{2A}$R and 5-HT$_{2B}$R co-expression in the pre-BötC and BötC suggests that, as in the pontine respiratory group, 5-HT$_{2A}$R modulation is predominant.

Differential effects of 5-HT$_{2A}$ and 5-HT$_{2B}$ receptor agonists and antagonists on phrenic nerve discharge properties

Activation of 5-HT$_{2A}$Rs by the selective, CNS-permeable agonist TCB-2 [47,56] increased PNA discharge amplitude but not frequency, whereas the 5-HT$_{2A}$R antagonist Altanserin decreased both amplitude and frequency: in fact, discharge frequency decreased below control level. Although speculative, we suggest that 5-HT$_{2A}$R agonists target two functionally different populations of respiratory neurons: bulbospinal inspiratory neurons, leading to increased phrenic motor output, and propriobulbar inspiratory phase-regulating neurons that determine discharge frequency.

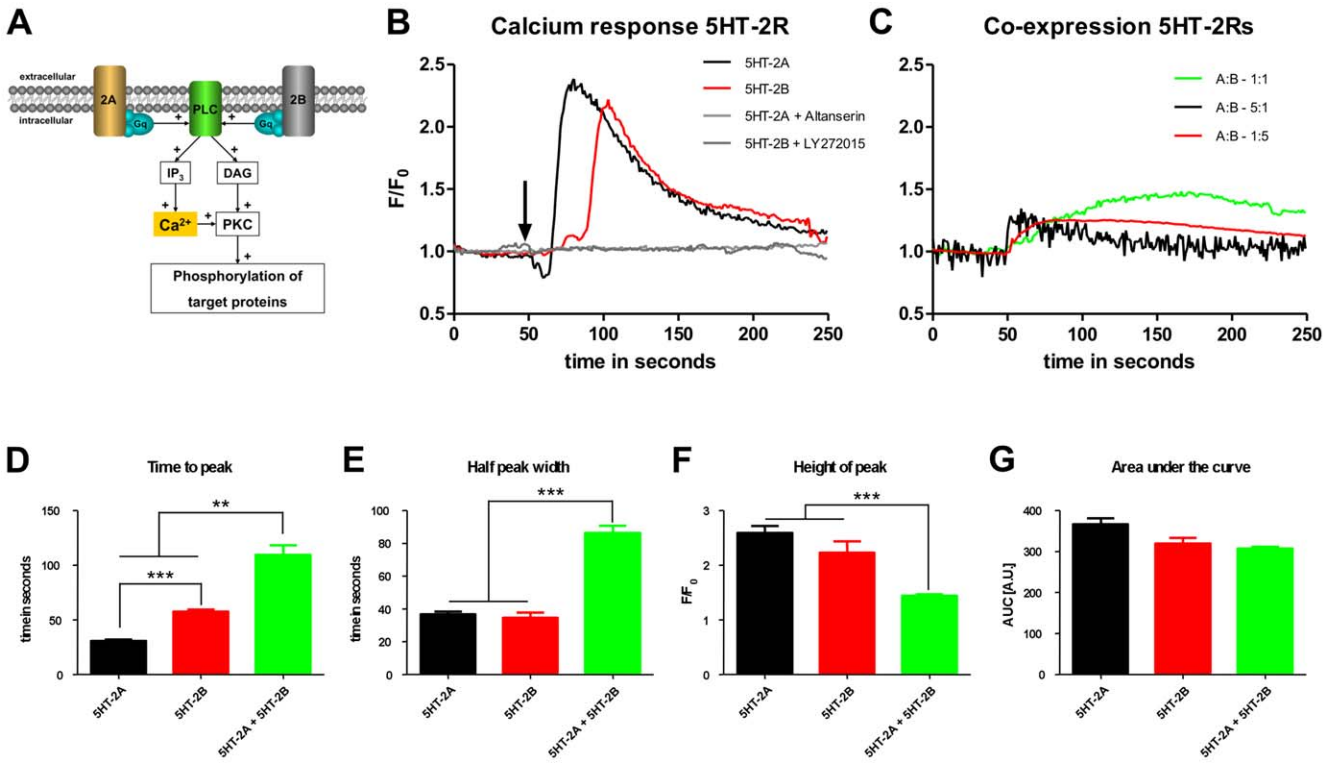

Figure 7. Signal transduction pathways of 5-HT$_{2A}$ and 5-HT$_{2B}$ receptors and calcium imaging. (**A**) The schematic diagram illustrates convergent signaling pathways for 5-HT$_2$Rs. (**B**) shows summed calcium transients recorded in N1E-115 cells transfected with either 5-HT$_{2A}$R (red line) or 5-HT$_{2B}$R (black line). The curves were constructed from the means of 3–5 independent experiments, averaging at least 30 individual measurements. The arrow indicates the time of stimulation. Light and dark grey curves indicate control experiments of 5-HT$_{2A}$R stimulated with Altanserin and 5-HT$_{2B}$R stimulated with LY272015, respectively. (**C**) shows summed calcium transients recorded in N1E-115 cells transfected with a stiochiometric ratio of 5-HT$_{2A}$R:5-HT$_{2B}$R of 1:1 (green line), 5-HT$_{2A}$R:5-HT$_{2B}$R of 5:1 (black line) and 5-HT$_{2A}$R:5-HT$_{2B}$R of 1:5 (red line). The bar diagrams (D–G) show statistical analysis of (**D**) height of peak (F/F$_0$), (**E**) time to peak (s), (**F**) half peak width (s) and (**G**) area under the curve (AU) for expression of 5-HT$_{2A}$R alone (black), 5-HT$_{2B}$R alone (red) or expression of 5-HT$_{2A}$R and 5-HT$_{2B}$R together at a stiochiometric ratio of 1:1 (green). Asterisks indicate significance (*** = $p<0.001$; ** = $p<0.01$; paired t-test). Abbreviations:, serotonin 2A receptor (2A), serotonin 2B receptor (2B), phospholipase C (PLC), inositol 1, 4, 5-triphosphate (IP$_3$), diacylglycerol (DAG), protein kinase C (PKC), hetero-trimeric guanine-nucleotide-binding protein q (G$_q$), adenylyl cyclase (AC), cyclic adenosine 5′, 3′-monophosphate (cAMP), protein kinase A (PKA).
doi:10.1371/journal.pone.0021395.g007

Altanserin's capacity to reduce discharge frequency below control levels indicates that constitutive 5-HT$_{2A}$R activation is substantial in inspiratory phase regulating neurons.

The 5-HT$_{2B}$R agonist BW 723C68 increased only frequency, indicating that only neurons involved in discharge rate regulation were affected. However, the antagonist LY 272015 changed neither amplitude nor frequency. This suggests that in our *in situ* perfused brainstem preparation, 5-HT$_{2B}$Rs though present and activated by BW 723C68 were not constitutively activated.

When 5-HT$_{2A}$R and 5-HT$_{2B}$R agonists were given concurrently, a frequency increase that exceeded the singular effects of either agonist occurred. This is an expected outcome if frequency-controlling neurons are preferred targets for 5-HT$_{2B}$R modulation in the ponto-medullary respiratory compartment.

5-HT$_{2B}$ and 5-HT$_{2A}$ receptors effects on Ca^{2+} signaling

Because 5-HT$_{2A}$ and 5-HT$_{2B}$ receptors both utilize an intracellular signal pathway that leads to a buildup of cytoplasmic

Table 1. Effects of 5-HT$_{2A}$R and 5-HT$_{2B}$R agonists on Ca^{2+} fluorescence signals.

Ca^{2+} Signal Properties	5-HT$_{2A}$R-agonist	5-HT$_{2B}$R agonist	both agonists	Unit	T-test*	T-test**
Onset time	10.1±1,7	40.3±1.5	11.9±2.3	[sec]	p, 0.001	p, 0.01[a]
Time to peak	30. 5±9.6	57.5±8.4	79.44±8.9	[sec]	p, 0.01	p, 0.01
Half peak width	36.7±1.7	34.6±3.2	86.32±5.0	[sec]	p, 0.500	p, 0.001
Height of peak (F/F$_0$)	2.59±0.8	2.23±1.1	1.44±0.17	[AU]	p, 0.500	p, 0.001
Area under the curve	366.38±93.64	319.4±74.86	307.43±24.43	[AU]	p, 0.500	p, 0.500

*comparing results from single transfected cells stimulated with 5-HT$_{2A}$R-agonist or with 5-HT$_{2B}$R agonist.
**comparing results from both single transfected/stimulated cells against double transfected/double stimulated cells.
[a]only when compared to single transfected cells stimulated with 5-HT$_{2A}$R.
doi:10.1371/journal.pone.0021395.t001

Ca^{2+}, we used the Ca^{2+} signal as a measure of receptor activation by TCB-2 and by BW 723C68. Neuroblastoma cells, for reasons presented earlier, are advantageous for measuring the magnitude and kinetics of intracellular Ca^{2+} fluctuations. Nonetheless, we acknowledge that there are limitations in relating Ca^{2+} signals detected in neuroblastoma cells to discharge properties recorded from the phrenic motor output, and we interpret our results with this caveat in mind.

Agonist activation of 5-HT_{2A} receptors produced a Ca^{2+} signal that was rapid in onset, somewhat faster in time course to peak and larger in magnitude than the Ca^{2+} transient produced by 5-HT_{2B} receptor activation. Another characteristic difference was an initial small dip in the signal due to 5-HT_{2A} receptors, whereas a small Ca^{2+} transient preceded the predominant 5-HT_{2B}R dependent signal. Their respective signal profiles may reflect differences in dynamic interactions involving receptor activation, cell membrane Ca-channel openings as well as Ca^{2+} release and uptake processes in intracellular organelles. A detailed interpretation of Ca^{2+} signals recorded from the respiratory rhythmic rodent slice preparation can be found in published studies by Keller and coworkers [57,58]. Those studies illustrate Ca^{2+} signals that are proportional to respiratory discharge intensity. Assuming that Ca^{2+} signaling in neuroblastoma cells can be equated with signaling in cells of the brainstem respiratory network, we interpret our findings as follows. The faster and larger Ca^{2+} signal may reflect more efficient 5-HT_{2A}R coupling to the PLC-DAG-PKC signal pathway, or to the spatial arrangement of receptor, Ca^{2+}-channel, and organelles involved in Ca^{2+} release and uptake. We can offer no ready explanation for the slowing and diminution of the Ca^{2+} signal when 5-HT_{2A} and 5-HT_{2B} receptors co-expressed in neuroblastoma cells were coactivated. Perhaps different isoforms of DAG or PKC activated by 5-HT_{2A}R and 5-HT_{2B}R compete for phosphorylation sites on membrane calcium channels and storage sites and interact negatively.

Conclusion

Taking together the results from all sets of experiments (distribution, co-expression, phrenic nerve activity, and Ca^{2+} signaling), we formulate the following working hypothesis: 5-HT_{2A}R is the dominant receptor governing respiratory control as evidenced by its stronger expression and constitutive activity. 5-HT_{2B}R, being present in all respiratory nuclei analyzed and co-expressed with 5-HT_{2A}R in many cells, although at a much reduced level, may act as a dose-dependent modulator. If more serotonin is released than needed to activate all 5-HT_{2A}Rs, 5-HT_{2B}Rs become activated. This would allow the system to regulate the respiratory rhythm by controlling serotonin release. Activation of spare 5-HT_{2B}R has the strongest effect on respiratory frequency. This regulation could, at least in part, be due to Ca^{2+} signaling, as the presence of 5-HT_{2B}R changes the kinetics of the Ca^{2+} signaling observed for both receptors alone, without altering the overall amount of mobilized calcium.

Author Contributions

Conceived and designed the experiments: TM SV MN. Performed the experiments: TM SV MN URK AMB MK. Analyzed the data: TM SV MN. Wrote the paper: TM MN NB.

References

1. Dick TE, Berger AJ (1985) Axonal projections of single bulbospinal inspiratory neurons revealed by spike-triggered averaging and antidromic activation. J Neurophysiol 53: 1590–603.
2. Holtman JR, Jr., Dick TE, Berger AJ (1986) Involvement of serotonin in the excitation of phrenic motoneurons evoked by stimulation of the raphe obscurus. J Neurosci 6: 1185–93.
3. Lalley PM (1986) Serotoninergic and non-serotoninergic responses of phrenic motoneurones to raphe stimulation in the cat. J Physiol 380: 373–85.
4. Millhorn DE, Hökfelt T, Verhofstad AA, Terenius L (1989) Individual cells in the raphe nuclei of the medulla oblongata in rat that contain immunoreactivities for both serotonin and enkephalin project to the spinal cord. Exp Brain Res 75: 536–42.
5. Holtman JR, Jr., Marion LJ, Speck DF (1990) Origin of serotonin-containing projections to the ventral respiratory group in the rat. Neuroscience 37: 541–52.
6. Lalley PM, Benacka R, Bischoff AM, Richter DW (1997) Nucleus raphe obscurus evokes 5-HT-1A receptor-mediated modulation of respiratory neurons. Brain Res 747: 156–9.
7. Richter DW, Lalley PM, Pierrefiche O, Haji A, Bischoff AM, et al. (1997) Intracellular signal pathways controlling respiratory neurons. Respir Physiol 110: 113–123.
8. Kubin L, Volgin DV (2008) Developmental profiles of neurotransmitter receptors in respiratory motor nuclei. Respir Physiol Neurobiol 164: 64–71.
9. Lalley PM, Bischoff AM, Richter DW (1994) Serotonin 1A-receptor activation suppresses respiratory apneusis in the cat. Neurosci Lett 172: 59–62.
10. El-Khatib MF, Kiwan RA, Jamaleddine GW (2003) Buspirone treatment for apneustic breathing in brain stem infarct. Respir Care 48: 956–958.
11. Wilken B, Lalley P, Bischoff AM, Christen HJ, Behnke J, et al. (1997) Treatment of apneustic respiratory disturbance with a serotonin-receptor agonist. J Pediatr 130: 89–94.
12. Manzke T, Guenther U, Ponimaskin EG, Haller M, Dutschmann M, et al. (2003) 5-HT4(a) receptors avert opioid-induced breathing depression without loss of analgesia. Science 301: 226–229.
13. Stettner GM, Zanella S, Hilaire G, Dutschmann M (2008) 8-OH-DPAT suppresses spontaneous central apneas in the C57BL/6J mouse strain. Respir Physiol Neurobiol 161: 10–15.
14. Yamauchi M, Ocak H, Dostal J, Jacono FJ, Loparo KA, et al. (2008a) Post-sigh breathing behavior and spontaneous pauses in the C57BL/6J (B6) mouse. Respir Physiol Neurobiol 162: 117–125.
15. Yamauchi M, Dostal J, Kimura H, Strohl KP (2008b) Effects of buspirone on posthypoxic ventilatory behavior in the C57BL/6J and A/J mouse strains. J Appl Physiol 105: 518–526.
16. Guenther U, Manzke T, Wrigge H, Dutschmann M, Zinserling J, Putensen C, et al. (2009) The counteraction of opioid-induced ventilatory depression by the serotonin 1A-agonist 8-OH-DPAT does not antagonize antinociception in rats in situ and in vivo. Anesth Analg 108: 1169–76.
17. Manzke T, Dutschmann M, Schlaf G, Mörschel M, Koch UR, et al. (2009) Serotonin targets inhibitory synapses to induce modulation of network functions. Philos Trans R Soc Lond B Biol Sci 364: 2589–602.
18. Hoyer D, Clarke DE, Fozard JR, Hartig PR, Martin GR, et al. (1994) International Union of Pharmacology classification of receptors for 5-hydroxytryptamine (Serotonin). Pharmacol Rev 46: 157–203.
19. Hoyer D, Hannon JP, Martin GR (2002) Molecular, pharmacological and functional diversity of 5-HT receptors. Pharmacol Biochem Behav 71: 533–554.
20. Palacios JM, Waeber C, Hoyer D, Mengod G (1990) Distribution of serotonin receptors. Ann N Y Acad Sci 600: 36–52.
21. Cornea-Hebert V, Riad M, Wu C, Singh SK, Descarries L (1999) Cellular and subcellular distribution of the serotonin 5-HT2A receptor in the central nervous system of adult rat. J Comp Neurol 409: 187–209.
22. Vergé D, Calas A (2000) Serotoninergic neurons and serotonin receptors: gains from cytochemical approaches. J Chem Neuroanat 18: 41–56.
23. Wright IK, Garratt JC, Marsden CA (1990) Effects of a selective 5-HT2 agonist, DOI, on 5-HT neuronal firing in the dorsal raphe nucleus and 5-HT release and meta-bolism in the frontal cortex. Br J Pharmacol 99: 221–222.
24. Garratt JC, Kidd EJ, Wright IK, Marsden CA (1991) Inhibition of 5-hydroxytryptamine neuronal activity by the 5-HT agonist, DOI. Eur J Pharmacol 199: 349–355.
25. Lalley PM, Bischoff AM, Schwarzacher SW, Richter DW (1995) 5-HT2 receptor-controlled modulation of medullary respiratory neurones in the cat. J Physiol 487: 653–661.
26. Haji A, Pierrefiche O, Lalley PM, Richter DW (1996) Protein kinase C pathways modulate respiratory pattern generation in the cat. J Physiol 494: 297–306.
27. Onimaru H, Shamoto A, Homma I (1998) Modulation of respiratory rhythm by 5-HT in the brainstem-spinal cord preparation from newborn rat. Pflugers Arch 435: 485–494.
28. Kinkead R, Bach KB, Johnson SM, Hodgeman BA, Mitchell GS (2001) Plasticity in respiratory motor control: intermittent hypoxia and hypercapnia activate opposing serotonergic and noradrenergic modulatory systems. Comp Biochem Physiol A Mol Integr Physiol 130: 207–218.
29. Baker-Herman TL, Mitchell GS (2002) Phrenic long-term facilitation requires spinal serotonin receptor activation and protein synthesis. J Neurosci 22: 6239–6246.

30. Lovett-Barr MR, Mitchell GS, Satriotomo I, Johnson SM (2006) Serotonin-induced in vitro long-term facilitation exhibits differential pattern sensitivity in cervical and thoracic inspiratory motor output. Neuroscience 142: 885–892.
31. Mahamed S, Mitchell GS (2008) Simulated apnoeas induce serotonin-dependent respiratory long-term facilitation in rats. J Physiol 586: 2171–2181.
32. Kennett GA, Wood MD, Bright F, Cilia J, Piper DC, et al. (1996) In vitro and in vivo profile of SB 206553, a potent 5-HT2C/5-HT2B receptor antagonist with anxiolytic-like properties. Br J Pharmacol 117: 427–434.
33. Callebert J, Esteve JM, Hervé P, Peoc'h K, Tournois C, et al. (2006) Evidence for a control of plasma serotonin levels by 5-hydroxytryptamine(2B) receptors in mice. J Pharmacol Exp Ther 317: 724–731.
34. Nebigil CG, Choi DS, Dierich A, Hickel P, Le Meur M, et al. (2000) Serotonin 2B receptor is required for heart development. Proc Natl Acad Sci 97: 9508–9513.
35. Günther S, Maroteaux L, Schwarzacher SW (2006) Endogenous 5-HT2B receptor activation regulates neonatal respiratory activity in vitro. J Neurobiol 66: 949–961.
36. Duxon MS, Flanigan TP, Reavley AC, Baxter GS, Blackburn TP, et al. (1997) Evidence for the expression of the 5-HT2B receptor protein in the rat central nervous system. Neuroscience 76: 323–329.
37. Smith JC, Ellenberger HH, Ballanyi K, Richter DW, Feldman JL (1991) Pre-Bötzinger complex: a brainstem region that may generate respiratory rhythm in mammals. Science 254: 726–729.
38. Connelly CA, Dobbins EG, Feldman JL (1992) Pre-Botzinger complex in cats: respiratory neuronal discharge patterns. Brain Res 590: 337–340.
39. Schwarzacher SW, Smith JC, Richter DW (1995) Pre-Bötzinger complex in the cat. J Neurophysiol 73: 1452–1461.
40. Feldman JL, Mitchell GS, Nattie EE (2003) Breathing: rhythmicity, plasticity, chemosensitivity. Annu Rev Neurosci 26: 239–266.
41. Pfaffl MW (2001) A new mathematical model for relative quantification in real-time RT-PCR. Nucleic Acids Res 29: e45.
42. Bedlack RS, Wei M, Fox SH, Gross E, Loew LM (1999) Distinct electric potentials in soma and neurite membranes. Neuron 13(5): 1187–1193.
43. Xu C, Loew LM (2003) Activation of Phospholipase C Increases Intramembrane Electric Fields in N1E-115 Neuroblastoma Cells. Biophys J 84(6): 4144–4156.
44. Paton JF (1996) A working heart-brainstem preparation of the mouse. J Neurosci Methods 65: 63–8.
45. Sietnicks A (1985) Involvement of 5-HT_2 receptors in the LSD- and L-5-HTP-induced suppression of lordotic behavior in the female rat. J Neural Transm 61: 65–80.
46. Audia JE, Evrard DA, Murdoch GR, Droste JJ, Nissen JS, et al. (1996) Potent, selective tetrahydro-beta-carboline antagonists of the serotonin 2B (5-HT_{2B}) contractile receptor in the rat stomach fundus. J Med Chem 39: 2773–80.
47. McLean TH, Parrish JC, Braden MR, Marona-Lewicka D, Gallardo-Godoy A, et al. (2006) 1-Aminomethylbenzocycloalkanes: conformationally restricted hallucino-genic phenethylamine analogues as functionally selective 5-HT2A receptor agonists. J Med Chem 49: 5794–803.
48. Alheid, McCrimmon (2008) The chemical neuroanatomy of breathing. Respir Physiol Neurobiol 164: 3–11.
49. Fay R, Kubin L (2000) Pontomedullary distribution of 5-HT2A receptor-like protein in the rat. J Comp Neurol 418: 323–45.
50. Ezure K, Tanaka I (2006) Distribution and medullary projection of respiratory neurons in the dorsolateral pons of the rat. Neuroscience 141: 1011–1023.
51. Song G, Yu Y, Poon CS (2006) Cytoarchitecture of pneumotaxic integration of respiratory and nonrespiratory information in the rat. J Neurosci 26(1): 300–310.
52. Pierrefiche O, Schwarzacher SW, Bischoff AM, Richter DW (1998) Blockade of synaptic inhibition within the pre-Botzinger complex in the cat suppresses respiratory rhythm generation in vivo. J Physiol 509: 245–254.
53. Feldman JL, Janczewski WA (2006) Point:Counterpoint: The parafacial respiratory group (pFRG)/pre-Botzinger complex (preBotC) is the primary site of respiratory rhythm generation in the mammal. Counterpoint: the preBötC is the primary site of respiratory rhythm generation in the mammal. J Appl Physiol 100(6): 2096–2097; discussion 2097–2098.
54. Jiang C, Lipski J (1990) Extensive monosynaptic inhibition of ventral respiratory group neurons by augmenting neurons in the Bötzinger complex in the cat. Exp Brain Res 81(3): 639–648.
55. Tian GF, Peever JH, Duffin J (1998) Bötzinger-complex expiratory neurons monosynaptically inhibit phrenic motoneurons in the decerebrate rat. Exp Brain Res 122(2): 149–156.
56. Fox MA, French HT, Laporte JL, Blackler AR, Murphy DL (2009) The serotonin 5-HT(2A) receptor agonist TCB-2: a behavioral and neurophysiological analysis. Psychopharmacology;DOI 10.1007/s00213-009-1694-1.
57. Lips MB, Keller BU (1999) Activity-related calcium dynamics in motoneurons of the nucleus hypoglossus from mouse. J Neurophysiol 82: 2936–2946.
58. Ladewig T, Keller BU (2000) Simultaneous patch-clamp recording and calcium imaging in a rhythmically active neuronal network in the brainstem slice preparation from mouse. Pflugers Arch 440: 322–332.